vided that the application in question has a magnitude of the transfer function which approximately equals unity, i.e.

$$|S_{21}|_0 \simeq 1 \quad (12)$$

these expressions are

$$IM_{2\omega_1-\omega_2} = \frac{V_s^2}{4mg^2\omega_1|(\omega_1-\omega_2)^2-\omega_m^2|}\left|\frac{\partial S_{21}}{\partial X}\right|_{\omega_1} \quad (13)$$

$$IM_{2\omega_1+\omega_2} = \frac{V_s^2}{4mg^2\omega_1}\left(\frac{1}{(\omega_1+\omega_2)^2}\left|\frac{\partial S_{21}}{\partial X}\right|_{\omega_1}+\frac{1}{8\omega_1\omega_2}\left|\frac{\partial S_{21}}{\partial X}\right|_{\omega_2}\right) \quad (14)$$

$$IM_{3\omega} = \frac{V_s^2}{32mg^2\omega^3}\left|\frac{\partial S_{21}}{\partial X}\right|_{\omega} \quad (15)$$

From these expressions, it is clear that the intermodulation product with the angular frequency $2\omega_1 - \omega_2$ has the highest level. Note also that, for eqn. 13 to be valid, the separation between the tones should not be close to the beam mechanical resonance frequency.

Switch application: For a certain design, the transfer function S_{21} is first found, and its derivative with respect to the switch reactance. As an example, expressions for spurious frequency component magnitudes are found for a single non-actuated switch on a transmission line. Such a switch is modelled with a variable shunt capacitor on a transmission line with characteristic impedance Z_0. The derivative of the transfer function S_{21} for this case, assuming the magnitude of X is much larger that Z_0, is

$$\left|\frac{\partial S_{21}}{\partial X}\right|_{\omega} \simeq \frac{Z_0}{2X^2} = \frac{Z_0\varepsilon^2A^2\omega^2}{2g^2} \quad (16)$$

Using eqn. 16 together with eqns. 4, 6 and 7, and replacing the angular frequency with frequency f, the expression for the modulation is found to be (in decibels)

$$M = 20\log\left(\frac{\pi Z_0\varepsilon A f\Delta g}{2g^2}\right) \quad (17)$$

Looking at intermodulation, if the input power per tone is P, the voltage V_s is

$$V_s = \sqrt{2PZ_0} \quad (18)$$

Inserting eqn. 16 into eqns. 13 – 15, and with angular frequencies replaced with corresponding frequencies, the expressions for intermodulation products and harmonics are (in decibels)

$$IM_{2f_1-f_2} = 20\log\left(\frac{PZ_0^2\varepsilon^2A^2f_1}{8\pi mg^4|(f_1-f_2)^2-f_m^2|}\right) \quad (19)$$

$$IM_{2f_1+f_2} = 20\log\left(\frac{PZ_0^2\varepsilon^2A^2}{8\pi mg^4}\left(\frac{f_1}{(f_1+f_2)^2}+\frac{f_2}{8f_1^2}\right)\right) \quad (20)$$

$$IM_{3f} = 20\log\left(\frac{PZ_0^2\varepsilon^2A^2}{64\pi mg^4f}\right) \quad (21)$$

Note that in eqns. 19 – 21 g is the average gap with the RF signal present. Since there is a DC component in the RF signal squared, this gap is less than the relaxed gap g_0. The actual value of g is calculated from eqns. 1 and 2 with

$$V = \frac{V_s}{\sqrt{2}} \quad (22)$$

for the case of a single tone, and

$$V = V_s \quad (23)$$

for the case of two simultaneous tones, each with amplitude V_s.

Conclusions: Mechanically or electrically induced beam motion in certain types of MEMS switches can cause problems of spurious frequency components. Main issues are modulation by mechanical resonance oscillations of the beam, and RF third-order intermodulation of the type $2f_1 - f_2$. The frequency separation between two RF tones simultaneously passing a switch should not be close to the mechanical resonance frequency of the switch.

26 March 2001
Electronics Letters Online No: 20010476
DOI: 10.1049/el:20010476

P. Hallbjörner (*Ericsson Research, Corporate Unit, Ericsson Microwave Systems AB, SE-431 84 Mölndal, Sweden*)

E-mail: paul.hallbjorner@emw.ericsson.se

J.P. Starski (*Chalmers University of Technology, Department of Microelectronics ED, SE-412 96 Göteborg, Sweden*)

References

1 BROWN, E.R.: 'RF-MEMS switches for reconfigurable integrated circuits', *IEEE Trans. Microw. Theory Tech.*, 1998, **46**, (11) pp. 1868–1880
2 YAO, Z.J., CHEN, S., ESHELMAN, S., DENNISTON, D., and GOLDSMITH, C.: 'Micromachined low-loss microwave switches', *IEEE J. Microelectromech. Syst.*, 1999, **8**, (2) pp. 129–134
3 CHENG, D.K.: 'Field and wave electromagnetics' (Addison-Wesley, 1989), 2nd edn., Chap. 3, pp. 133–143
4 BUECHE, F.J.: 'Introduction to physics for scientists and engineers' (McGraw-Hill, 1986), 4th edn., Chap. 10, p. 216

Microstrip ring resonator using quarter-wave couplers

C.E. Saavedra

A microstrip ring resonator that uses quarter-wave coupled lines for input and output coupling is presented. The ring exhibits a double resonance due to an asymmetry in the topology of the structure. When the asymmetry is removed a single resonant peak is observed. The insertion loss of the ring is 6dB and its quality factor is 64.

Introduction: Ring resonators have found use in a variety of applications such as oscillators [1], tuned amplifiers [2], filters [3], and microwave substrate characterisation [4]. Recent work [5 – 9] on microstrip rings has focused on using enhanced coupling mechanisms. In this Letter, a ring resonator that uses quarter-wave ($\lambda/4$) edge-coupled lines as the coupling mechanism is investigated. Special attention is devoted to the physical structure of the ring to eliminate dual modes, which manifest themselves as a double-resonance in the frequency response of the ring.

Square ring resonator with strong coupling: A square ring resonator with input and output $\lambda/4$ couplers is depicted in Fig. 1*a*. The ring was etched on a substrate with a relative dielectric constant of 2.2 and a thickness of 0.127 mm. The length of each side of the ring is 3.65 mm, and the coupling gap is 0.1 mm. The width of the transmission lines and the resonator strip is 0.38 mm, which corresponds to a 50 Ω impedance for the substrate used.

The frequency response of the ring was measured with a vector network analyser using a thru-reflect-line (TRL) calibration to de-embed the coaxial-to-microstrip transition of the test fixture. The results are plotted in Fig. 1*b*. The double resonance at 14.24 and 14.45 GHz can be explained by considering the topology of the ring. Referring to Fig. 1*a*, the impedance of the ring in regions 1 and 3 differs from that of regions 2 and 4 because the coupled lines load the ring. The ring structure in Fig. 1 is not symmetric about the x or y axes which leads to the split-resonant behaviour because two modes are excited in the ring [8, 9].

Symmetric ring resonator: When the ring is loaded with coupled lines on all four sides, as depicted in Fig. 2*a*, the structure becomes essentially symmetric and the double-resonance disappears since the impedance is uniform throughout the structure. The measured frequency response of the ring is shown in Fig. 2*b*. The key features that distinguish this ring resonator from other rings that use strong coupling mechanisms are its relatively low insertion loss and high quality factor (Q-factor). For the ring under consideration, the insertion loss is -6.0 dB at the resonant frequency of 14.4 GHz. Using the expression

$$Q = \omega_0/\Delta\omega$$

where ω_0 is the resonant frequency and $\Delta\omega$ is the 3 dB bandwidth, the Q-factor is found to be 64. The quality factor can be further increased at the expense of insertion loss by weakening the coupling in and out of the ring. This is achieved by increasing the gap between the ring and the input and output transmission lines. The gap between the ring and the $\lambda/4$ lines in regions 2 and 4 has to increase by the same amount in order to preserve the symmetry of the ring.

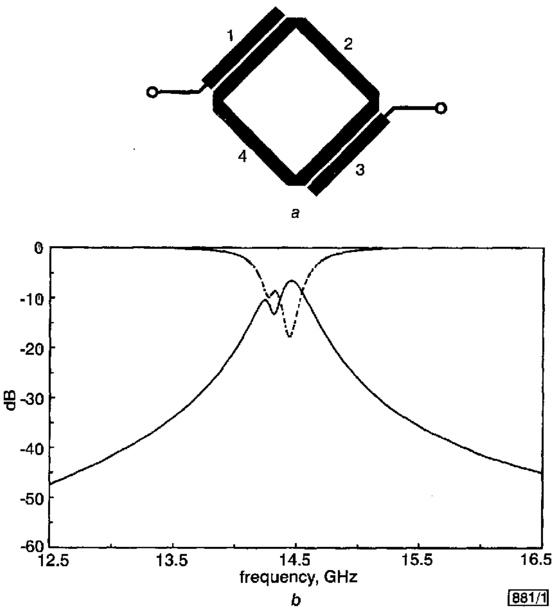

Fig. 1 *Square ring resonator with quarter-wave coupling mechanism and frequency response*

a Square ring resonator
b Frequency response
– – – – return loss
——— insertion loss

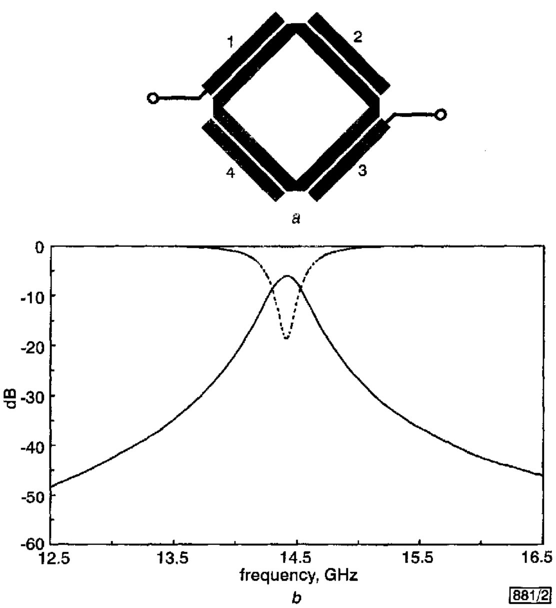

Fig. 2 *Symmetric resonator and frequency response*

a Symmetric resonator
b Frequency response
– – – – return loss
——— insertion loss

To predict the resonant frequency of a square ring resonator, the effect of the mitered bends has to be taken into account. To a first approximation, the bends add a length of line, *l*, to each side of the resonator. For a ring, the resonant length is given by the expression

$$\lambda_r = \frac{c}{\sqrt{\varepsilon_{eff}} f_r}$$

where *c* is the speed of light, f_r is the resonant frequency, and ε_{eff} is the effective dielectric constant. For the ring in Fig. 2*b* this expression yields λ_r = 15.11 mm using ε_{eff} = 1.88. Therefore, the mitered ends add a length l = [15.18 mm − 4*(3.65 mm)]/4 = 0.128 mm to each side of the ring.

Conclusions: Microstrip ring resonators using a strong coupling mechanism have been investigated. If the resonator is asymmetric, resonance splitting is observed because dual modes are excited in the structure. The asymmetry of the structure can be removed by loading the ring around its entire periphery with coupled lines.

2 April 2001
Electronics Letters Online No: 20010482
DOI: 10.1049/el:20010482

C.E. Saavedra (*Department of Electrical and Computer Engineering, Queen's University, Kingston, Ontario, K7L 3N6 Canada*)

References

1 CHANG, K., MARTIN, S., WANG, F., and KLEIN, J.L.: 'On the study of microstrip ring and varactor-tuned ring circuits', *IEEE Trans. Microwave Theory Tech.*, 1987, **MTT-35**, (12), pp. 1288–1295
2 YABUKI, H., SAGAWA, M., MATSUO, M., and MAKIMOTO, M.: 'Stripline dual-mode ring resonators and their application to microwave devices', *IEEE Trans. Microwave Theory Tech.*, 1996, **44**, (5), pp. 723–728
3 TROUGHTON, P.: 'Measurement techniques in microstrip', *Electron. Lett.*, 1969, **5**, (2), pp. 25–26
4 MATTHAEI, G., YOUNG, L., and JONES, E.M.T.: 'Microwave filters, impedance-matching networks, and coupling structures' (Artech House, 1980)
5 ZHU, L., and WU, K.: 'A joint field/circuit model of line-to-ring coupling structures and its application to the design of microstrip dual-mode filters and ring resonator circuits', *IEEE Trans. Microw. Theory Tech.*, 1999, **47**, (10). pp. 1938–1948
6 PARK, J.-Y., and LEE, J.-C.: 'A new enhanced coupling structure of microstrip ring resonator with two coupled lines and a slit'. 1998 IEEE MTT-S Dig., 1998, pp. 805–808
7 GOPALAKRISHNAN, G.K., and CHANG, K.: 'Novel excitation schemes for the microstrip ring resonator with lower insertion loss', *Electron. Lett.*, 1994, **30**, (2), pp. 148–149
8 WESTED, J., and ANDERSEN, E.: 'Resonance splitting in nonuniform ring resonators', *Electron. Lett.*, 1972, **8**, (12), pp. 301–302
9 WOLFF, I.: 'Microstrip bandpass filter using degenerate modes of a microstrip ring resonator', *Electron. Lett.*, 1972, **8**, (12), pp. 302–303

Burst-error-correcting algorithm for Reed-Solomon codes

Liuguo Yin, Jianhua Lu, K. Ben Letaief and Youshou Wu

A new decoding algorithm for burst-error-correction is proposed. The proposed algorithm can effectively correct burst errors of length approaching $n - k$ symbols for (n, k) Reed-Solomon (RS) codes. Compared with existing algorithms, the algorithm enables much faster decoding with far less computational complexity.

Introduction: Reed-Solomon (RS) codes have been proven to be very effective in correcting burst errors, whereas conventional decoding algorithms often assume that the occurrence of a symbol error is independent of that of others, and burst errors are treated as the same as random errors in the decoding procedure. According to the Singleton bound, the maximum length of burst errors that can be corrected by a (n, k) RS code is $(n - k)/2$. Recent stud-